Geologia Sudetica, 1998, 31: 93–104.

Orthogneisses and metapelites from a polyphase tectonic zone - mesostructural versus microstructural evidence: an example from the Czerniawa Zdrój section (Izera-Karkonosze Block, West Sudetes)

Wojciech Czapliński

Instytut Nauk Geologicznych PAN, Podwale 75, 50-449 Wrocław, Poland, e-mail: wojtekcz@twarda.pan.pl

Key words: West Sudetes, Izera–Karkonosze Block, microstructures, quartz *c*-axis

Abstract Within the gneisses of the northern part of the Izera–Karkonosze Block (West Sudetes), there are 4 belts of schistose rocks. The Stara Kamienica schist belt in the Czerniawa section consists of a sequence of orthogneisses deformed to various degree, occurring concordantly with metapelitic mica schists. Structural analysis of these rocks, including quartz *c*-axis analysis, allows four stages of deformation, common for both lithologies to be recognized. The quartz *c*-axis microfabrics are often incompatible with other elements of the structural record, which is interpreted as having resulted from multiple overprinting of older microfabrics by younger ones in a heterogeneous deformation regime. This heterogeneity concerns the geometry of the deformation as well as the mechanisms, which included subgrain-rotation recrystallization, grain-boundary migration, microfracturing and pressure-solution processes.

Manuscript received: 17 November 1997, accepted: 27 May 1998.

INTRODUCTION

This paper presents the results of a structural study of two lithologically and rheologically contrasting neighbouring rock units, which were deformed during the same tectonic events in the same P–T conditions and kinematic framework. In the area of study, an almost continuous profile across a sequence of granite mylonites (further in this paper referred also to as intra-schist gneisses), contacting concordantly with metapelitic mica schists crops out. The rocks are deformed to a variable degree.

The objective of this study was to check the degree of compatibility between observed meso- and microstructures with evolving quartz *c*-axis microfabrics. Numerous theoretical and experimental works, combined with studies of naturally deformed rocks have cleared up the relationships between the *c*-axis microfabrics and active slip systems, type and magnitude of finite strain and strain path (e. g. Lister & Williams, 1979; Schmid & Casey, 1986; MacCready, 1996).

The method employed was the analysis of quartz *c*-axis microfabrics compared with routine structural analysis of structures, kinematic indicators and metamorphic changes of minerals. The observations show limited compatibility and the reasons for that are discusssed.

GEOLOGICAL SETTINGS

The examined rocks belong to the Stara Kamienica schist belt unit (referred to from now as the Kamienica belt), which is an arcuate, E–W trending schistose belt transecting the Izera gneisses (Fig. 1), part of the northern margin of the Bohemian Massif. From the east and west the Kamienica Belt is cut by the Variscan Karkonosze granite intrusion. To the north the Kamienica belt is bordered by the Izera gneisses, while to the south either by gneisses or by leucocratic rocks of metasomatic origin (Kozłowski, 1974). The penetrative foliation of the Kamienica belt rocks is parallel to its boundaries and to the general trend of foliation in the Izera gneisses, dipping to the north at moderate to steep angles. The lithology of this unit includes various types of quartz–mica schists, embed-

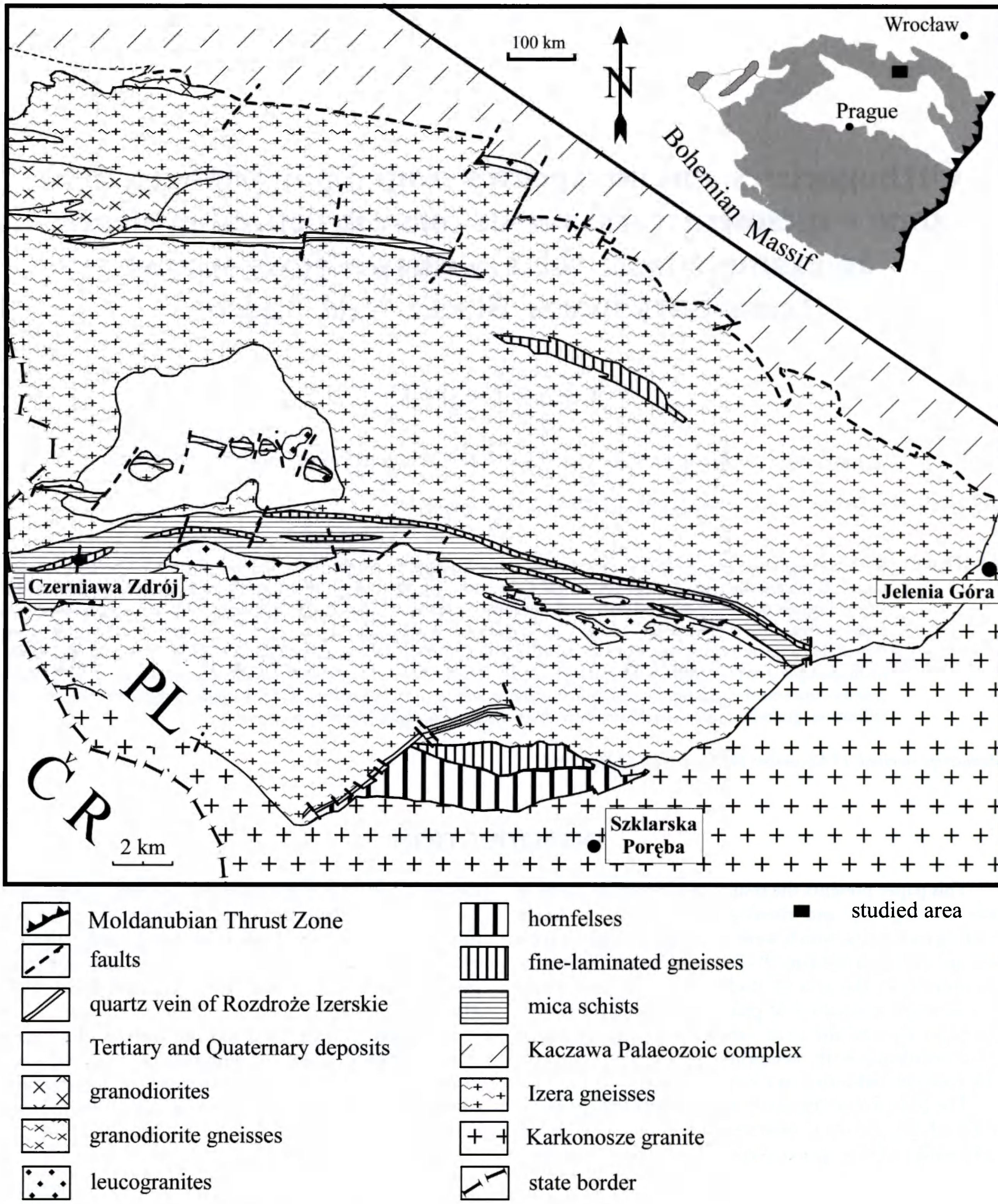

Fig. 1. General map of the Izera-Karkonosze Block (after Mierzejewski & Oberc-Dziedzic, 1990)

ding concordant bodies (of various size) of gneisses and, less often amphibolites, quartzites and calc–silicate rocks. Some horizons of the schists are enriched in chloritoid, garnet and/or Sn-Co-Ni-As-Bi mineralization (*cf.* Cook & Dudek, 1994). The occurrence of kyanite, reported by Jaskólski & Mochnacka (1958) and Szałamacha & Szalamacha (1968) was not confirmed. It was most probably chloritoid mistaken for kyanite.

The Izera gneisses, the host rocks of the Kamienica belt, are of magmatic origin and their age datings are: 480–450 Ma (Rb-Sr whole rock; Borkowska *et al.*, 1980) and 515–490 Ma (U-Pb zircon; Korytowski *et al.*, 1993;

Philippe *et al.*, 1995). Datings from the metapelites have yet to be done.

The mica schists of the Kamienica belt were metamorphosed at peak metamorphic conditions estimated in the range: 470–620°C and 3,5–9 kbar (Żaba, 1985; Cook & Dudek, 1994; Makała, 1994).

The intra-schist gneisses are the most conspicuous element of the Kamienica belt internal structure, since they occur along almost half of its strike as a concordant inlier of varying width. So far, little attention was paid to these rocks and their origin and tectonic history remain unclear. According to Berg (1926) they constitute apophyses of the main magmatic body of the Izera granites. Other workers (Smulikowski, 1972; Kozłowski, 1974) assumed their metasedimentary origin.

The area of study is located in Czerniawa Zdrój, along the eastern bank of the Czarny stream (Fig. 2).

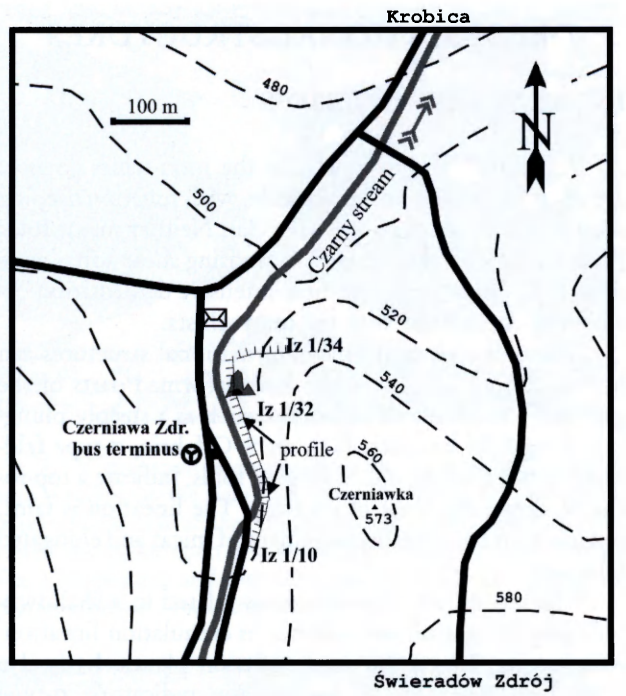

Fig. 2. Location of the Czerniawa Zdrój section

PETROGRAPHY

INTRA-SCHIST GNEISSES

The intra-schist gneisses are finely laminated (thickness of the quartz and quartzo -feldspatic laminae: 0.5–5 mm, micaceous laminae: 0.1–1 mm), with small feldspar augen. In the studied profile, towards the contact with the metapelitic mica schists, the gneisses gradually become more schistose in appearance, due to their very fine lamination and the strong mica lustre on the foliation planes.

The mineral composition of the intra-schist gneisses is monotonously granitic: quartz + feldspars (K-feldspar and oligoclase) + micas (predominantly white mica) + accessories (opaques, apatite, zircon). With the increasing degree of deformation (= grain size and foliation spacing reduction) the total feldspar content gradually decreases, while the bulk content of quartz + micas increases.

The K-feldspar porphyroclasts are more or less rounded, sometimes with narrow (usually only a few grains thick) mantles of recrystallized, fine-grained microcline-albite aggregate. The cores suffer from various retrograde alterations, among which sericitization, causing their "dusty" appearance, is the most common. Another common type of alteration is the formation of chequered albite. The feldspars are often cross-cut by zones of recrystallized material and/or fractures. The fine-grained feldspars from the matrix are equant and angular or rounded. The former are usually microclines, the latter – albites. Some feldspar grains exhibit deformation twinning, flame perthites or rarely undulatory extinction.

Muscovite is present in the least deformed samples as isolated grains or parallelly aligned aggregates. With the increasing degree of deformation, the micaceous laminae become better pronounced and in the most deformed samples they constitute the penetrative foliation (compositional layering). Simultaneously, due to retrograde metamorphic reactions, the bulk content of muscovite increases.

Biotite, also parallel to foliation, is much less abundant than muscovite but ubiquitous. Zircon inclusions surrounded by pleochroic haloes are very common. Biotite is usually chloritized to various degree.

Quartz veins of various scale are usually concordant with the foliation. Observed at mesoscopic scale, small sheared veinlets are almost indistinguishable from the "normal" quartz laminae.

In the case of a very high degree of deformation, a mesoscopic distinction between gneiss-derived mylonite and metapelitic mica schist is extremely difficult. However careful examination, even with the naked eye, reveals the presence of feldspar porphyroclasts, diagnostic for the gneisses.

METAPELITIC MICA SCHISTS

Mesoscopically the metapelitic schists from Czerniawa Zdrój are very finely laminated, with "leafy" schistosity and characteristic silvery or greenish lustre.

The petrography of these schists is very variable. Across a relatively short section of the Czerniawa profile, quartz–muscovite, quartz–muscovite–chlorite, quartz–muscovite–biotite and quartz–muscovite–biotite–chlorite schists occur. The penetrative foliation is defined by alternating quartz and mica laminae, often only one grain thick. Some horizons are enriched in garnets (almandine – Szałamacha & Szałamacha, 1974), chloritoid and/or opaques (mainly rutile in various stages of replacement by sphene). In some sections accessory feldspar (small relics) was observed.

Chlorite is abundant, usually replacing biotite, but also occuring as a late mineral, sometimes even filling small veinlets cross-cutting the penetrative foliation.

Numerous generations of quartz veins occur in various forms (lenses, veins *sensu stricto*) and are both concordant with and discordant to the foliation.

DEFORMATIONAL STRUCTURES

INTRA-SCHIST GNEISSES

At individual outcrops scale the intra-schist gneisses are deformed rather homogenously, with foliation dipping monotonously to the north (Fig. 3a). Neither major folds (above 0.5 meter scale) nor anastomosing shear zones were observed. The zone of the most intensive deformation occurs near the contact with the mica schists.

The oldest recognizable deformational structures can be found only locally, in the least deformed parts of the gneisses. The observed structures, such as a steeply plunging elongation lineation (L_1), an S–C fabric, σ-type feldspar porphyroclasts and N-verging folds, indicate a top-to-the-N, down-dip sense of shearing. The lineation is faint, pronounced by a parallel alignment of micas and elongated feldspars.

The second set of structures is related to a shallowly plunging elongation and sometimes crenulation lineation, overprinting L_1 on the same foliation planes. L_2 is also weakly pronounced. The kinematic indicators: σ-type feldspar porphyroclasts (Fig. 4), V-pull-aparts (Fig. 5; see Hippertt, 1993) and the grain shape fabric of the quartz veinlets, indicate a top-to-the-W (sinistral) sense of shearing.

The third set of structures is observable in sections parallel to L_2. It is not possible to determine whether L_3 was not formed or it is parallel to L_2. The recognized structures: σ-type felsdpar porphyroclasts, the grain shape fabric of the quartz veinlets and S–C fabrics indicate top-to-the-E (dextral) shearing.

The fourth set of structures is related to the widespread, SSW/SW-verging kink-folds. The slickensides on their limbs also show a SSW sense of displacement. A crenulation cleavage, parallel to their axial planes developed locally.

Besides the above mentioned asymmetric kinematic indicators, also ϕ-type porphyroclasts (with tails symmetrical with respect to the foliation) and symmetrically pulled-apart fragments of feldspar porphyroclasts occur very commonly. The space between displaced feldspar fragments is usually filled by quartz.

MICA SCHISTS

The most prominent structural feature of the mica schists is a very densely spaced penetrative foliation, parallel to that in the intra-schist gneisses (Fig. 3b). It seems that this foliation, at least in some horizons, although enhanced by shearing, basically resulted from the transposition of an earlier planar feature (sedimentary bedding?). This can be evidenced by the occurrence of the older foliation relicts (Fig. 6).

No kinematic indicators have been found, which could be related without any doubt to the first generation of deformational structures in the intra-schist gneisses (top-to-the-N, down-dip displacement). Inclusion trails enclosed in garnet (Fig. 7) are the best candidate, but they are

a)

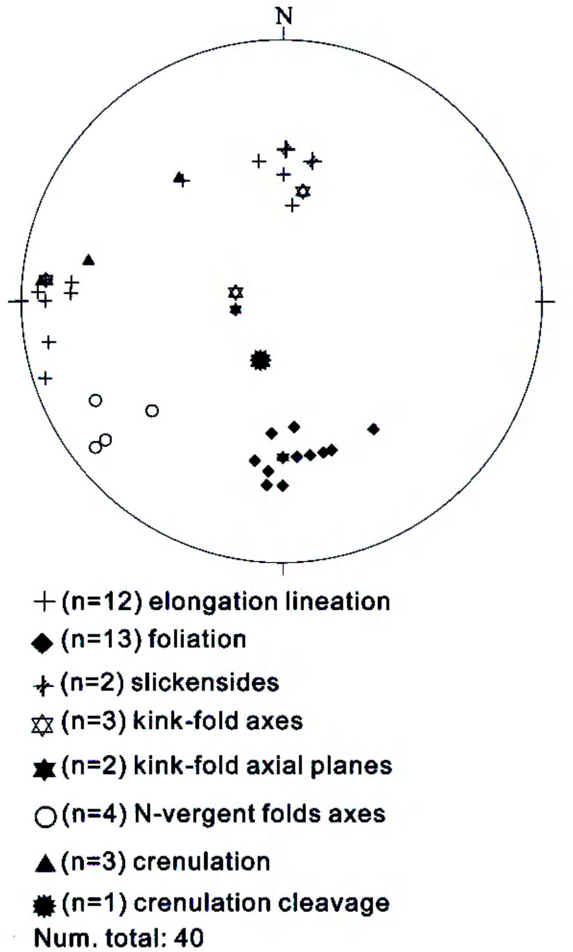

b)

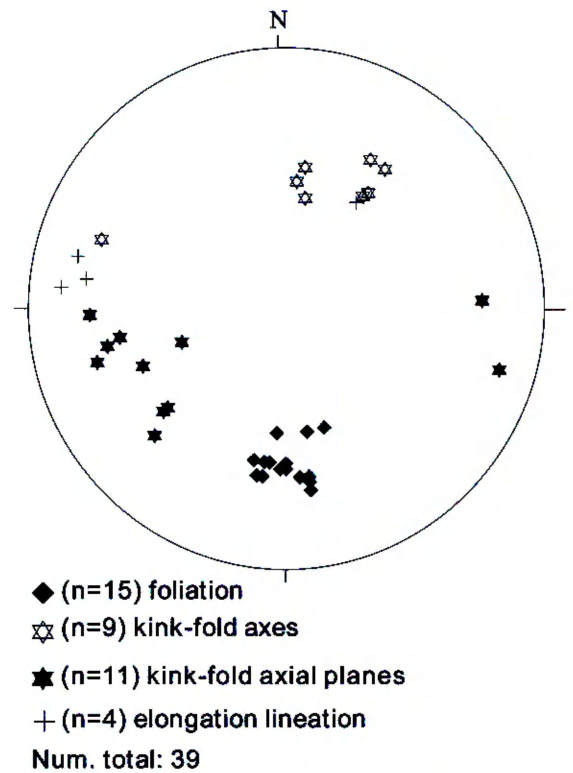

Fig. 3. Orientation of tectonic structures: a) in the intra-schist gneisses; b) in the metapelites

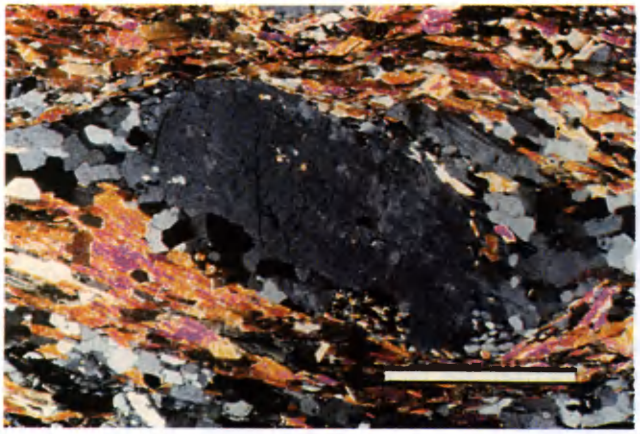

Fig. 4. K-feldspar σ-type porphyroclast with recrystallized tails indicating "top-to-the-W" sense of shear; scale bar 1 mm; crossed polarizers

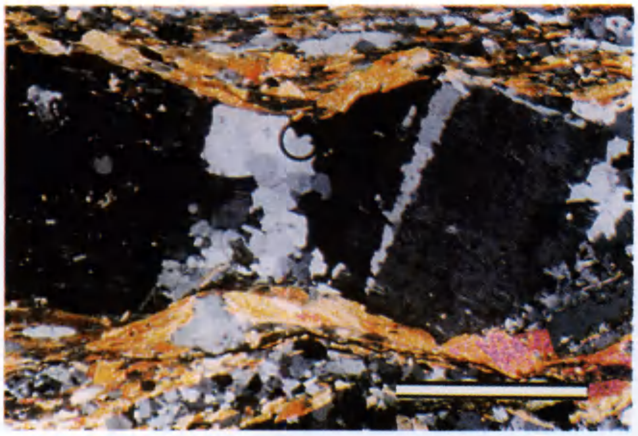

Fig. 5. 'V'-pull-apart microstructure: the fragment of the feldpar porphyroclast on the right-hand side was rotated clockwise with respect to the rest of the "mother" grain. The fragment in the middle was pulled-apart symmetrically, which implies extension. The V-shaped gap and the wider gap to the left are filled with quartz; scale bar 1 mm; crossed polarizers

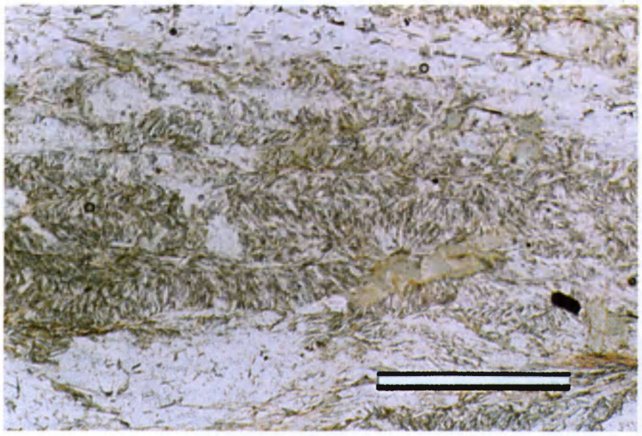

Fig. 6. Transposition of the older, S_0 mimetic foliation (subvertical), into penetrative S_1 metamorphic foliation (horizontal) in metapelites; scale bar 1 mm; one polarizer

Fig. 7. Spiral inclusion trail in garnet (in non-ideal section) formed during D_1; asymmetric pressure shadows, composed of chlorite and quartz were formed during D_2 (sinistral shearing); scale bar 1 mm; crossed polarizers

unfortunately only found in non-ideal section. The asymmetric pressure shadows at that garnet, composed of quartz and chlorite, indicate top-to-the-W shearing, associated with a subhorizontal lineation. They are correlated with D_2 structures in the gneisses. In sections other then those with accessory garnets, the kinematic indicators are rare and poorly developed. They usually occur in the form of small drag folds (deforming quartz veinlets) and sigmoidal mica fish, often indicating opposite senses of shear in the same samples.

The mica schists are locally intensively folded by at least two sets of kink-bands. In some localities clear overprinting relationships can be observed, while in the others the kink-bands seem to constitute conjugate systems.

QUARTZ MICROFABRICS

MICROSTRUCTURES

The quartz grains from both the gneisses and the mica schists can be divided into two groups:

1) porphyroclasts and recrystallized new grains;

2) grains from the deformed veinlets;

In the gneisses, the first type includes grains of various size (0.1 mm–1mm), generally decreasing in size with an increasing degree of deformation. Similarly the grains shape changes from irregular through polygonal to equant. With an increasing degree of deformation in the metapelites both the grain size and grain shape are more uniform. The grain boundaries are slightly irregular or straight. Undulatory extinction and optical subgrains are the rule.

Grains of the second type are generally large (1

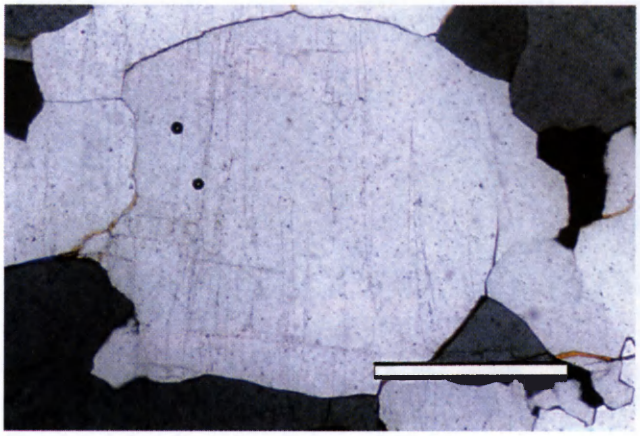

Fig. 8. Inclusion trails in quartz aligned along crystallographic planes: subvertical parallel to prism planes, horizontal parallel to basal planes; scale bar 0.5 mm; crossed polarizers

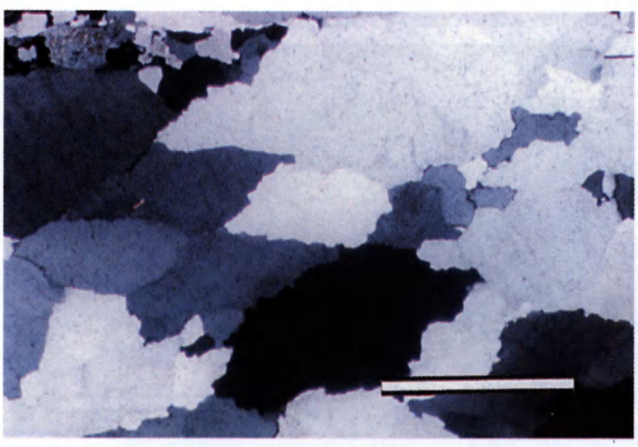

Fig. 9. Oblique alignment of quartz grain boundaries defining the shape fabric; the sense of obliquity (S_1 foliation horizontal) is consistent with "top-to-the-E" sense of shear established from independent kinematic indicators; scale bar 1 mm; crossed polarizers

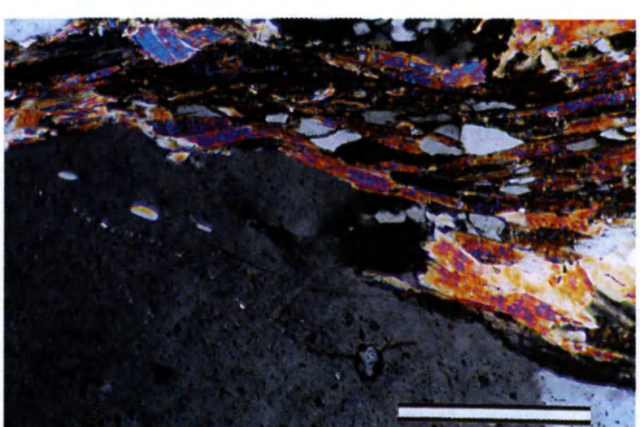

Fig. 10. Dissolution–precipitation driven truncation of the quartz grain leading to smoothening of quartz–mica lamina boundary. Note the alignment of inclusions and sericite flakes along the quartz basal planes (from upper left to lower right); scale bar 0.2 mm; crossed polarizers

mm–3.5 mm), irregular in shape, with highly lobate or serrated boundaries. Optical subgrains are rare. A very distinctive feature is the presence of numerous inclusion trails (Fig. 8). The often parallel alignment of grain boundaries in this type defines shape fabric (Fig. 9).

Both in the gneisses and mica schists, along the contacts with the micaceous domains the quartz grain boundaries are usually straight, in the convex parts showing symptomps of pressure-solution driven truncation (Fig. 10). This phenomenon of selective dissolution of quartz along the basal planes and its replacement by muscovite was described by Hippertt (1993) as one of the major mechanism forming the metamorphic foliation in phyllonites.

QUARTZ C-AXIS PREFERRED ORIENTATION

Thin sections for quartz *c*-axis measurements were cut from planes perpendicular to the foliation and parallel to the elongation lineation L_x (assumed to contain the XZ plane of the finite strain ellipsoid). When two lineations were present, the younger one, assumed to be related to fabric-forming deformation, was chosen. The number of measurements varied from section to section depending on the quartz content. Sections Iz 1/10 to Iz 1/29 were cut from gneisses and sections Iz 1/30 to Iz 1/34 from mica schists. Quartz *c*-axis orientations were measured on the universal stage and the measurements data was processed (contouring, rotating) using the stereonet software.

Most of the sections yielded interpretable quartz *c*-axis microfabrics, which are presented in Figure 11. However, some of the diagrams present almost random scatter (Iz 1/12/1), other resemble patterns obtained from sections perpendicular to the elongation lineation (Iz 1/16/1, Iz 1/31/1). In those cases, the incorrect measurement planes were suspected. Therefore, additional measurements were performed: from planes parallel to the older lineation , or – when it was absent – perpendicular to the lineation visible in the hand sample. Concurrently, for comparison, the original *c*-axis pole diagrams were rotated into parallelism with those additionally measured. The original diagrams are shown in the 1st column of figure 12, the orientations measured from perpendicular planes in the 2nd column and the rotated original data in the 3rd column. The sense of shearing, established from meso- and microstructures is displayed in the figures by thick arrows.

The most conspicuous *c*-axis pole figure was obtained from section Iz 1/10/1. This section was cut parallel to the subvertical lineation L_1, from the least deformed gneiss, as evidenced by the mean feldspar grain-size (Fig. 13) and contains kinematic indicators showing top-to-N, down-dip sense of shear. The skeletal outline can be interpreted as a Type I crossed girdle (Lister, 1977). Strongly populated maxima II (nomenclature after Fairnbairn, 1949) are the best pronounced "topographic" features of this *c*-axis pole figure.

Two other microfabrics obtained from sections Iz 1/11/1 and Iz 1/28/1 parallel to L_1, from the gneiss, can be

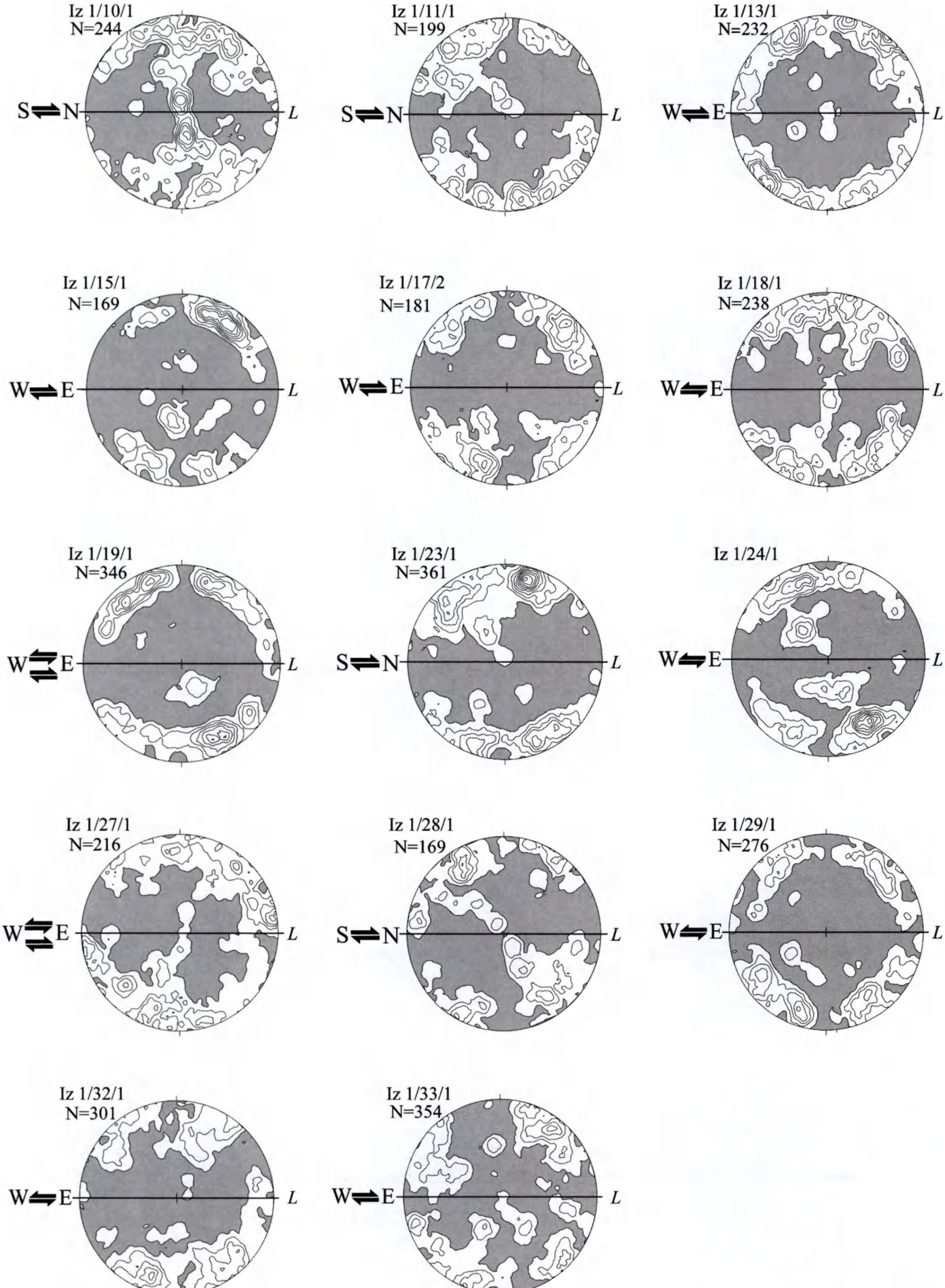

Fig. 11. Quartz *c*-axis original orientation diagrams; all data measured from the X-Z plane of the finite strain elipsoid

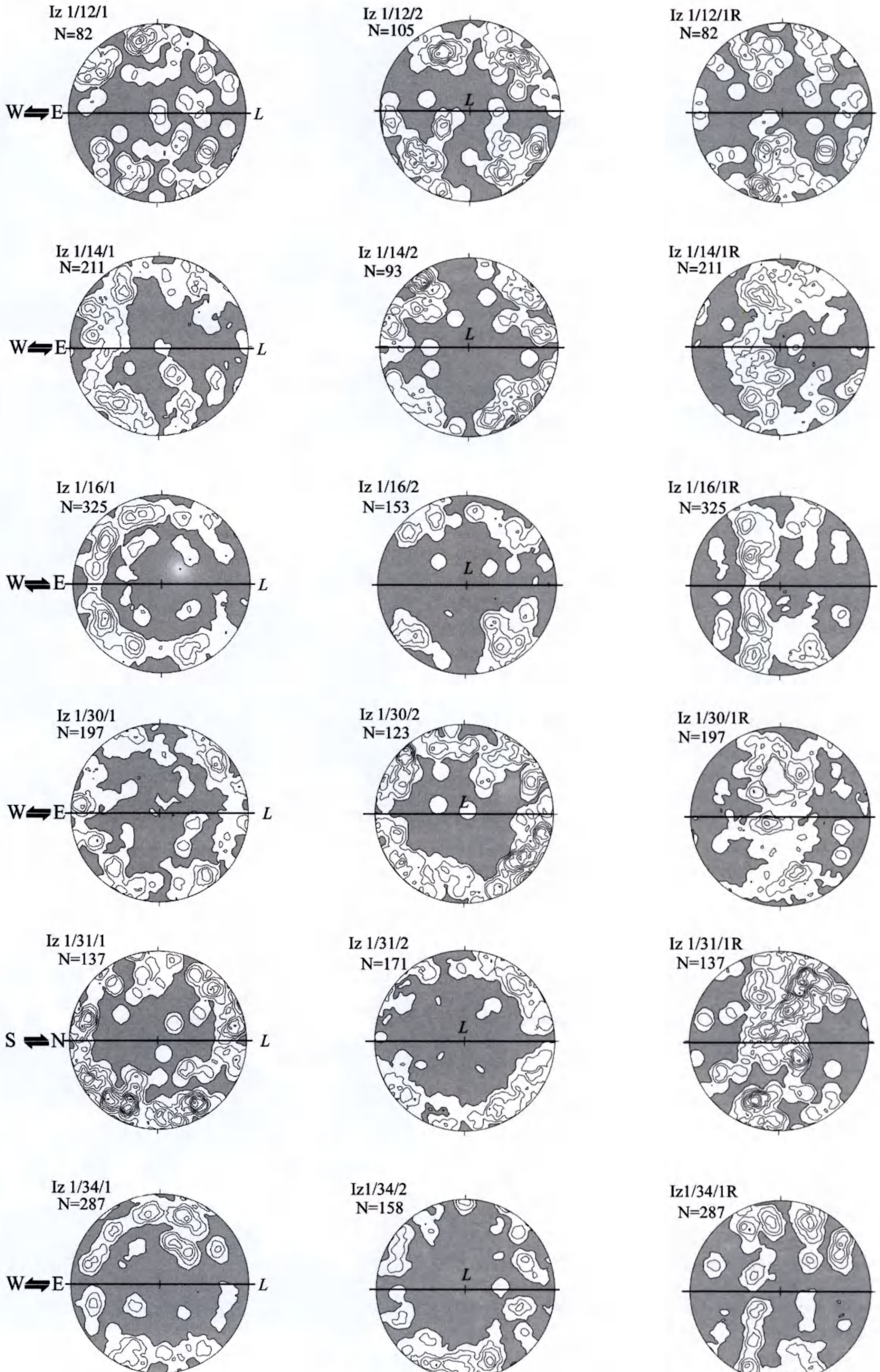

Fig. 12. Quartz *c*-axis orientation diagrams: 1st column – original measurements; 2nd column – additional measurements from planes perpendicular to the folation and the measurement plane of column 1; 3rd column – plots of original data rotated into parallelism with diagrams from column 2

interpreted as Type II crossed girdles with stronger maxima III and relict joining girdles. These girdles are populated asymmetrically in both cases and the stronger one is inclined towards the south. Diagram Iz 1/23/1, also obtained from the gneiss, from a section parallel to L_1, can be interpreted ambigously. Its lower half resembles a small circle around the foliation pole, while the upper half resembles asymmetrically populated maxima III. The stronger maximum is located on the northern side of diagram, which is consistent with the sense of shear displayed by the kinematic indicators present.

Only one diagram, Iz 1/31/1, was obtained from the mica schist from a section cut parallel to the subvertical lineation (Fig. 12). The original c-axis pole figure is uninterpretable. An additional measurement yielded weak, broad maxima III. Rotated original data show a broad, irregular single girdle perpendicular to the foliation.

Diagrams obtained from sections cut parallel to the subhorizontal lineation L_2 display mostly strongly populated maxima III and relict joining girdles. However some of these apparently orthorhombic fabrics show internal sense of asymmetry caused by a stronger maximum, a pair of maxima or stronger girdle. On diagrams Iz 1/15/1 and Iz 1/17/2 (obtained from gneisses) the internal sense of asymmetry is consistent with the top-to-E sense of shear established from kinematic indicators. Diagram Iz 1/33/1 (obtained from mica schist) also displays asymmetrically populated maxima, consistent with top-to-the-E sense of shear.

Diagrams Iz 1/19/1 and 1/27/1 (both from gneiss) contain kinematic indicators showing opposite senses of shear. The distribution of maxima in Iz 1/19/1 indicates top-to-the-W, while in Iz1/27/1 a top-to-the-E sense of asymmetry.

Diagram Iz 1/18/1 is interpreted as a Type I crossed girdle. It was obtained from a mylonitic gneiss, from a section parallel to L_2 and showing kinematic indicators displaying a top-to-W sense of shear. Its best pronounced "topographic" features are maxima III.

Diagram Iz 1/32/1, interpreted here as small circles around the foliation poles was obtained from a mica schist, from section parallel to the subhorizontal lineation. This section contains kinematic indicators showing a top-to-the-W sense of shear.

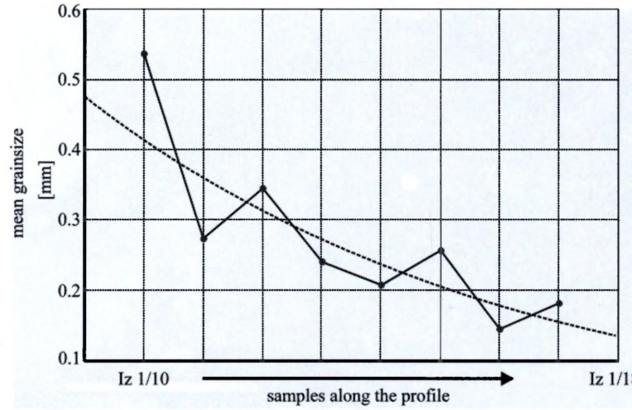

Fig. 13. Plot of the mean grain-size of feldspars from the intra-schist gneisses

The additional measurements (shown in the 2nd column of Fig. 12), perpendicular to the original data (1st column), mostly yielded Type II crossed girdles with strong maxima III and relict joining girdles. Such microfabrics obtained from gneisses are represented by diagrams Iz 1/12/2, Iz 1/14/2 and Iz 1/16/2. Microfabrics of this type obtained from the mica schists are represented by diagram Iz 1/31/2. The remaining microfabrics obtained from the mica schists, Iz 1/30/2 and Iz 1/31/2, are practically uninterpretable.

The *c*-axis pole figures resulting from rotation of the original data are variable, displaying great circles parallel to the YZ plane of the stereonet (Iz 1/16/1R, Iz 1/34/1R), a single broad girdle parallel to the YZ plane (Iz 1/14/1R, Iz 1/30/1R, Iz 1/31/1R) and almost random scatter (Iz 1/12/1R). It should be noted, that in no case the additionally measured quartz c-axis orientations are identical with those resulted from rotation of the original data.

HISTORY OF DEFORMATION

The relationships observed between deformational structures in the studied rocks alow the following sequence of deformations to be reconstructed:

D_1 – "top-to-the-north" shearing in a normal faulting regime;

D_2 – "top-to-the-west" shearing in a sinistral strike-slip regime;

D_3 – "top-to-the-east" shearing in a dextral strike-slip regime;

D_4 – "top-to-the-south-southwest" shearing in a oblique thrusting regime;

The onset of D_1 took place under lower amphibolite facies temperature conditions, as evidenced by the deformational behaviour of feldspars and strong maxima II on the *c*-axis pole figure (Iz 1/10/1 in Fig. 11). Maxima II are formed by dominant activity of the rhomb glide system during quartz deformation, which is commonly interpreted as indicative of the lower amphibolite facies temperature conditions (Schmid & Casey, 1986).

The deformation events $D_{2\text{-}4}$ went on during retrogression under greenschists facies conditions. This is inferred from the internally asymmetric microfabrics with dominant maxima III and relict joining girdles (e. g. Iz 1/19/1, Iz 1/24/1 in Fig. 12). Maxima III result from the basal glide system, active in the low-temperature deformation of quartz (Schmid & Casey, 1986). The semi-brittle behaviour of feldspars and formation of flame perthites (Fig. 14) also point to this temperature estimation (Pryer, 1995). D_4 took place at the lower temperature limit of the greenschists facies, as inferred from the formation of kink-

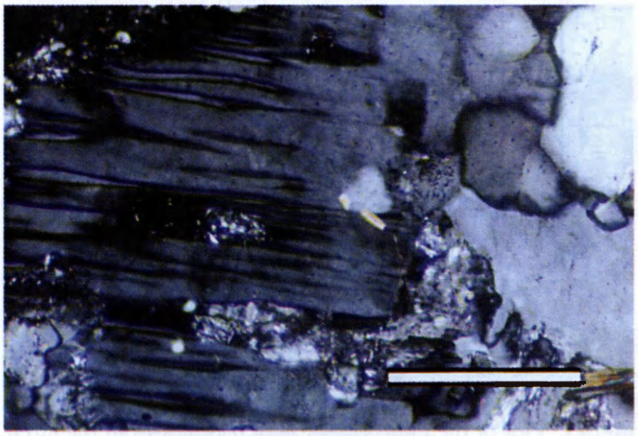

Fig. 14. Flame perthites in K-feldspar; scale bar 0.1 mm; crossed polarizers

folds during this phase.

The structural framework of the Kamienica belt was established probably during the tectonic event D_1 which emplaced the metapelites into their present position within the Izera gneisses. The mylonitic fabric was formed during D_1 and subsequent deformation events took place with S_1 acting as a pre-existing, rheologically soft anisotropy plane, which "channelled" later rocks displacements. During D_{2-4} both gneisses and mica schists were already deformed together, in the same kinematic framework and metamorphic conditions. D_1 in the mica schists may have resulted in extensive folding, forming the penetrative foliation in the axial planes of folds, or these folds may have been inherited from an earlier event. Such a large scale folding was assumed as D_1 in metapelites by Dziemiańczuk & Dziemiańczuk (1982). Although there are no major folds (except kink-bands) observed in the Czerniawa section, they are common in other parts of the Kamienica belt and many workers (e. g. Koszela, 1972; Żaba, 1984; Żaba & Teper, 1989) inferred the presence of tight isoclinal megafolds of hundreds of meters'amplitude. According to Koszela (1972), the garnet-bearing horizons represent in fact a single layer, repeated within the folds hinges.

The current position of the intra-schists gneisses probably results from the tectonic emplacement of Izera granite slivers into the metapelitic complex during D_1 faulting. Similar finely-laminated gneisses were reported to be in contact with the mica schists along the northern boundary of Kamienica belt (Szałamacha & Szałamacha, 1964). Both intra-schists gneisses and the boundary gneisses constitute then more intensively deformed Izera gneisses. No evidence for an intrusive origin of the intra-schist gneisses (e. g. relicts of the contact zone) was found. Nevertheless, the possibility of the intrusive origin of the intra-schist gneiss cannot be ruled out – the contact zone may have been destroyed during deformation.

On the basis of diagram Iz 1/10/1, which is assumed to represent the oldest quartz *c*-axis microfabric, formed at the highest temperature recorded by the distribution of maxima, D_1 can be described as general shearing with a coaxial component in the plane strain field. The regimes of D_{2-4} deformation events are impossible to reconstruct due to complicated overprinting and obliterating of the older structures by younger ones, produced during deformation events of mutually opposite kinematics. The deformational structures (σ- and ϕ-porphyroclasts, symmetrically pulled-apart and rotated fragments of porphyroclasts) are both asymmetric and symmetric, which indicates a complex geometry of deformations. The rotational character is evident, but it was rather general shear then simple shear. Weakly developed stretching lineations and a lack of pervasive S–C fabrics imply rather low amount of the rotational component.

The most common, Type II skeletal outlines of quartz microfabrics, obtained from sections with evident asymmetric kinematic indicators, can be interpreted in two ways:

1) The first interpretation assumes a coaxial overprint over the earlier, asymmetric fabric. Reorientation of the quartz microfabrics by a late strain increment, leaving other kinematic indicators (e. g. tailed porphyroclasts) untouched, was predicted theoretically (Lister & Williams, 1979; Lister & Hobbs, 1980) and observed in a regional study (MacCready, 1996). The internal asymmetry of Type II crossed girdles described above would then represent remnants of the older, asymmetric microfabrics.

2) The second interpretation is based on the concept of heterogeneous deformation and strain partitioning. With bulk deformation of general shear type, it is possible to partition strain between the domains of dominant pure and simple shear. In the studied case, the component of simple shear would have been accomodated by easy glide on {001} crystallographic planes in phyllosilicates, while the pure shear component by deformation of the feldspathic and quartzose laminae.

THE MECHANISMS OF DEFORMATION

Several processes were involved in the deformations of the studied rocks, as inferred from a variety of microstructures. In the gneisses, the most important were dynamic recovery and recrystallization (of different types). Subgrain-rotation recrystallization (climb accomodated creep) produced optical subgrains within the quartz grains. Grain-boundary migration (GBM) recrystalization (diffusion creep) resulted in highly lobate and serrated grain boundaries, with window and pinning microstructures (Jessel, 1987; Fig. 15). GBM was also responsible for the shape fabric of the sheared veinlets. The feldspars were initially deformed by dynamic recrystallization (subgrain-rotation) producing weak core-mantle structures, later by microkinking and fracturing. Concurrently strain softening, mica-producing retrograde metamorphic reactions were active.

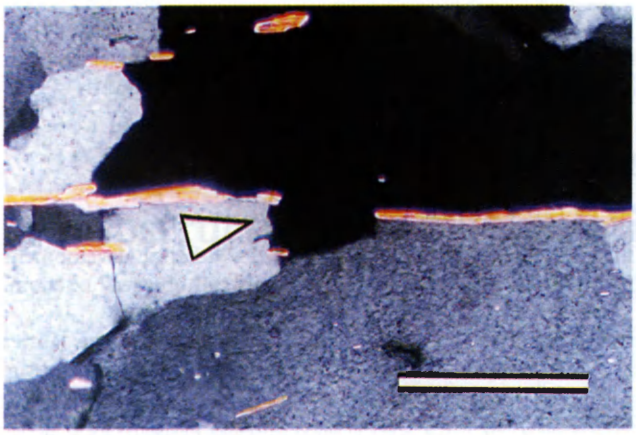

Fig. 15. "Window" microstructure, typical for grain-boundary migration; scale bar 0.2 mm; crossed polarizers

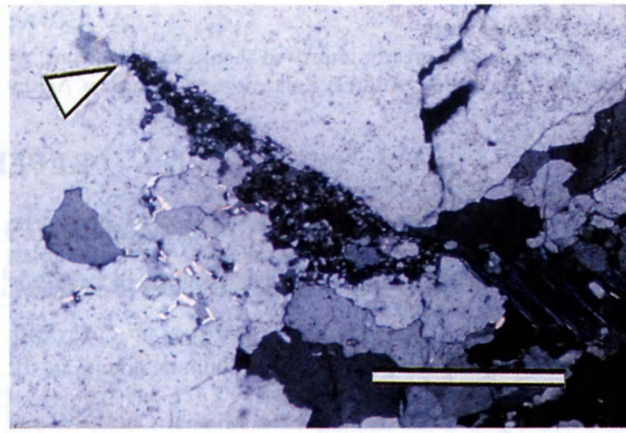

Fig. 16. Evidence for extensive dissolution-precipitation: array of the small quartz grains precipitated within a larger quartz grain; scale bar 0.5 mm; crossed polarizers

Mica schists were mainly deformed by intracrystalline slip on {001} plane in the phyllosilicates crystals and grain-boundary sliding. Nevertheless, some mechanisms of intra-crystalline slip in quartz were also active, producing preferred *c*-axis orientations. Intracrystalline slip on {001} in micas and grain boundary sliding was also probably active in the most deformed intra-schist gneisses.

Both gneisses and mica schists suffered from very intensive pressure-solution mass transfer, which is evidenced by abundant quartz veins, quartz precipitated between pulled-apart fragments of feldspars (Fig. 5), opaque accumulation in strain caps, selective replacement of quartz by mica and crystallization of the new quartz grains along the intragranular fractures (Fig. 16).

This complexity of deformational mechanisms may be responsible for the diffuse and unreadable quartz c-axis microfabrics. Gleason *et al.* (1993) suggest that quartz lattice preferred orientation depends strongly on the recrystallization mechanism. Grain boundary migration results in patterns different from those due to intracrystalline slip, which are commonly known from methodic papers and used as kinematic, geometric and temperature indicators (e. g. Schmid & Casey, 1986; Law, 1990). Hippertt (1994) observed the evolution of quartz *c*-axis microfabric through the various stages of deformation partitioning between crystal-plastic and transfer-solution processes. The microfabrics changed from Type I crossed girdles into girdles parallel to the stretching lineation through a stage of somewhat chaotic figures. That intermediate microfabric displayed maxima resulting from all glide systems possible in quartz.

The incompatibility of the quartz *c*-axis microfabrics from the 2nd and 3rd columns in Figure 12, indicates a high heterogeneity of deformation at hand samples scale. Assuming homogeneous deformation, the *c*-axis microfabrics measured from planes parallel to the elongation lineation, after 90 degree rotation should be identical to those measured from planes perpendicular to the elongation lineation.

CONCLUSIONS

The intra-schist gneisses and metapelitic mica schists were deformed together, in the same kinematic frames, during the following sequence of tectonic events:

D_1 – "top-to-the-north" shearing in a normal faulting regime;

D_2 – "top-to-the-west" shearing in a sinistral strike-slip regime;

D_3 – "top-to-the-east" shearing in a dextral strike-slip regime;

D_4 – "top-to-the-southsouthwest" shearing in a oblique thrusting regime;

The onset of D_1 took place under lower amphibolite facies conditions; subsequent deformations were undergone under retrograde greenschists facies, conditions. All movements were localized on S_1 ($=S_{2-4}$), the only penetrative foliation in the Czerniawa section and the common structural element of both gneisses and mica schists due to strain softening.

The deformations of the intra-schists gneisses and metapelites were accomplished by different dominant deformational mechanisms. In the gneisses the most important mechanisms were subgrain-rotation recrystallization and grain-boundary migration recrystallization, while in the metapelites gliding on phyllosilicates {001} crystallographic plane and grain-boundary sliding. In both lithologies a large fraction of the total strain was due to pressure-solution processes.

When analysing quartz *c*-axis microfabrics from polyphase tectonic zones, one should be aware of the numerous factors, potentially influencing the patterns which should originate from intracrystalline slip processes. All other available microstructural data should be taken into account.

Acknowledgments

This paper was greatly improved thanks to discussions, review and criticism by Andrzej Żelaźniewicz, Stanislaw Achramowicz and Dawid Bialek. Financial support was provided from Komitet Badań Naukowych, grant No. S602 030 06p01.

REFERENCES

BERG, G., 1926. *Erläuterungen zur Geologischen Karte von Preussen und benachbarten deutsches Ländern.* Blatt Flinsberg-Strickenhuser. Preussische Geologische Landesanstalt., Lieferung 262, Berlin.

BORKOWSKA, M., HAMEURT, J. & VIDAL, P., 1980. Origin and age of Izera granite and Rumburk granite in the Western Sudetes. *Acta Geol. Polon.*, 30: 121–145.

COOK, N. J. & DUDEK, K., 1994. Mineral Chemistry and Metamorphism of Garnet-Chlorite-Mica Schists Associated with Cassiterite - Sulphide Mineralization from the Kamienica Range, Izera Mountains, S. W. Poland. *Chemie der Erde*, 54: 1–32.

DZIEMIAŃCZUK, E. & DZIEMIAŃCZUK, K., 1982. Rozwój strukturalny lupków lyszczykowych Pasma Kamienieckiego między Czerniawą a Rębiszowem [Structural development of micaceous schists of the Pasmo Kamienieckie range between Czerniawa and Rębiszów]. *Kwart. Geol.*, 26: 13–43.

FAIRNBAIRN, H. W., 1949. *Structural petrology of deformed rocks*, Addison-Wesley, Cambridge, Massachusets.

GLEASON, G. C., TULLIS, J. & HEIDELBACH, F. 1993. The role of dynamic recrystalization in the development of lattice preferred orientations in experimentally sheared quartz aggregates. *J. Struct. Geol.*, 15: 1145–1168.

HIPPERTT, J. F. M., 1993. 'V'-pull-apart microstructures: a new shear-sense indicator. *J. Struct. Geol.*, 15: 1393–1403.

HIPPERTT, J. F. M., 1994. Microstructures and *c*-axis fabrics indicative of quartz dissolution in sheared quartzites and phyllonites. *J. Struct. Geol.*, 229: 141–163.

JASKÓLSKI, S. & MOCHNACKA, K., 1958. Zloże cyny w Gierczynie w Górach Izerskich na Dolnym Śląsku i próba wyjaśnienia jego genezy [Tin deposits at Gierczyn, in Iser Mountains, Lower Silesia, and attempt of elucidating their origin]. *Arch. Miner.*, 22: 17–106.

JESSEL, M. W., 1987. Grain-boundary migration microstructures in a naturally deformed quartzites. *J. Struct. Geol.*, 9: 1007–1014.

KORYTOWSKI, A., DÖRR, W. & ŻELAŹNIEWICZ A., 1993. U-Pb dating of (meta)-granitoids in the NW Sudetes (Poland) and their bearing on tectonostratigraphic correlation. *Terra Nova*, 5: 331–332.

KOSZELA, J., 1972. Mezoskopowe parakinematyczne struktury w lupkach lyszczykowych okolic Czerniawy Zdroju [Mesoscopic Parakinematic Structures in Mica Schists within the Czerniawa Zdrój Area]. *Kwart. Geol.*, 16: 37–51.

KOZLOWSKI, K., 1974. Łupki krystaliczne i leukogranity pasma Stara Kamienica-Świeradów Zdrój [Crystalline schists and leucogranites of the Stara Kamienica-Świeradów Zdrój Belt (Western Sudetes)]. *Geol. Sudetica*, 9: 7–98.

LAW, R. D., 1990. Crystallographic fabrics: a selective review of their applications to research in structural geology. In: Knipe, R. J. & Rutter, E. H. (Eds), *Deformation Mechanisms, Rheology and Tectonics*, Geol. Soc. London Spec. Publ., 54: 335–352.

LISTER, G. S., 1977. Crossed-girdle c-axis fabrics in quartzites plastically deformed by plane strain and progressive simple shear. *Tectonophysics*, 39: 51–54.

LISTER, G. S & HOBBS, B. E., 1980. The simulation of fabric development during plastic deformation and its application to quartzite: the influence of deformation history. *J. Struct. Geol.*, 2: 355–370

LISTER, G. S. & WILLIAMS, P. F., 1979. Fabric development in shear zones: theoretical controls and observed phenomena. *J. Struct. Geol.*, 1: 283–297.

MACCREADY, T., 1996. Misalignment of quartz c-axis fabrics and lineation due to oblique final strain increments in the Ruby Mountains core complex, *J. Struct. Geol.*, 18: 765–776.

MAKALA, A., 1994. Garnet-layer silicates paragenesis of metapelites from Stara Kamienica chain, Western Sudetes. *Arch. Miner.*, 50: 31–54.

MIERZEJEWSKI, M. P. & OBERC-DZIEDZIC, T., 1990. The Izera-Karkonosze Block and its tectonic development (Sudetes, Poland). *Neues Jahrb. Geol. Paläontol. Abhandl.*, 179: 197–222.

PHILIPPE, S., HAACK, U., ŻELAŹNIEWICZ, A., DÖRR, W. & FRANKE, W., 1995. Preliminary geochemical and geochronological results on shear zones in the Izera-Karkonosze Block (Sudetes, Poland). *Terra Nostra*, 8: 122.

PRYER, L. L. & ROBIN, P.-F., 1995. Retrograde metamorphic reactions in deforming granites and the origin of flame perthite. *J. Metamorphic Geol.*, 13: 645–658.

SCHMID, S. M. & CASEY, M., 1986. Complete fabric analysis of some commonly observed quartz c-axis patterns. In: Hobbs, B. E. & Heard, H. C. (Eds), *Mineral and Rock Deformation: Laboratory Studies, Am. Geophys. Union, Geophys. Monogr.*, 36: 263–286.

SMULIKOWSKI, W., 1972. Petrograficzne i strukturalne problemy pólnocnej okrywy granitu Karkonoszy [Petrogenetic and structural problems of the northern cover of the Karkonosze granite]. *Geol. Sudetica*, 6: 97–188.

SZALAMACHA, M. & SZALAMACHA, J., 1964. Problem pólnocnego kontaktu lupków lyszczykowych Pasma Starej Kamienicy z gnejsami Izerskimi. *Przegląd Geologiczny*, 7–8: 329–331 {in Polish only}.

SZALAMACHA, J. & SZALAMACHA, M., 1968. The metamorphic series of the Karkonosze-Góry Izerskie Mountain Block, *Biul. Inst. Geol.*, 222: 33–75.

SZALAMACHA, M. & SZALAMACHA, J., 1974. Geologiczna i petrograficzna charakterystyka lupków zmineralizowanych kasyterytem na przykladzie kamieniolomu w Krobicy [Geological and petrographic characteristic of schists mineralized with cassiterite on the basis of material from the quarry at Krobica]. *Biul. Inst. Geol.*, 279: 59–89

TULLIS, J. & WENK, H.-R., 1994. Effect of muscovite on the strenght and lattice preferred orientations of experimentally deformed quartz aggregates. *Materials Science and Engineering*, A175: 209–220.

ŻABA, J., 1984. Stosunek waryscyjskiego granitoidu Karkonoszy do metamorfiku pólnocnej oslony oraz tektonika faldowa pasm lupkowych Szklarskiej Poręby i Starej Kamienicy (krystalinik izerski). In: Żaba, J. (Ed.), *Zagadnienia tektoniki krystaliniku izersko-łużyckiego*, Uniwersytet Śląski, pp. 7–71 {in Polish only}.

ŻABA, J., 1985. Progressive regional metamorphism of the Izera Block, Western Sudetes (Poland). *Acta Universitas Carolinae, Geologica*, 1: 63–88.

ŻABA, J. & TEPER, L., 1989. Tectonic transport directions in the Izera Block (West Sudetes). *Krystalinikum*, 20: 131–150.